Soft Matter

Cite this: *Soft Matter*, 2011, **7**, 10951

www.rsc.org/softmatter

PAPER

Effect of rod–rod interaction on self-assembly behavior of ABC π-conjugated rod–coil–coil triblock copolymers

Chun-Jie Chang,[a] Yi-Huan Lee,[a] Hsin-Lung Chen,[b] Chien-Hung Chiang,[c] Hsiu-Fu Hsu,[c] Chun-Chih Ho,[d] Wei-Fang Su[ad] and Chi-An Dai*[ae]

Received 19th May 2011, Accepted 25th July 2011
DOI: 10.1039/c1sm05926b

A new class of ABC π-conjugated rod–coil–coil triblock copolymers of poly(diethylhexyloxy-*p*-phenylene vinylene)-*b*-poly (2-vinyl pyridine)-*b*-polystyrene (PPV-PVP-PS) was synthesized and its self-assembly behavior was explored. Three different triblock copolymers of PPV-PVP-PS1, PPV-PVP-PS2, and PPV-PVP-PS3, each with PPV, PS, and PVP, respectively, as the major species in the copolymers, were used to study the effects of copolymer composition and rod–rod interaction between PPV blocks on their morphology. Transmission electron microscopy (TEM), polarizing optical microscopy (POM), and simultaneously measured small-angle (SAXS) and wide-angle (WAXS) X-ray scattering experiments as a function of different annealing conditions revealed the details of the copolymer morphology, molecular packing, and their phase transitions. Despite their large differences in the rod volume fraction, f_{PPV}, from 0.43 to 0.18, all three triblock copolymers adopted a self-assembled lamellar structure, in sharp constrast with the observation of many non-lamellar structures typically exhibited by ABC coil–coil–coil triblock copolymers with similar segregation strength. For PPV-PVP-PS1 with its major species PPV rod coupled with a single-phase symmetric PVP-PS diblock precursor, PPV-PVP-PS1 self-organized to form a triple-lamellar phase with each domain corresponding to the three respective blocks. Investigation of the molecular packing of PPV rods within their domain through the analysis of the 1D electron density profile suggests the PPV rods adopted a smectic C monolayer organization below its order–disorder transition temperature (T_{ODT}). For PPV-PVP-PS2 with its PS-rich asymmetric PVP-PS diblock precursor that displayed a disordered micelle structure, PPV-PVP-PS2 with f_{PPV} of only 0.19 still exhibited a triple-lamellar phase with PPV forming a broken lamellar layer, thus preventing the excessive chain stretching of the coil blocks on the otherwise long-range ordered PPV lamellar phase. A similar broken triple-lamellar phase can also be observed for the PVP-rich PPV-PVP-PS3 with a low f_{PPV} of only 0.18. Simultaneous SAXS and WAXS measurements show that all three triblock copolymers undergo the ordered lamella-to-disorder transition and the smectic/isotropic transition at the same temperature, indicating that the rod–rod interaction between PPV rods plays a critical role in forming and stabilizing these lamellar structures. The observation of the phase transformations is in good agreement with a recent mean-field prediction of a rod–coil–coil triblock copolymer system.

Introduction

The self-assembly of diblock copolymers, which have a coil-like chain conformation for each constituent block, into nanostructures with diverse morphologies and novel properties has long been a subject of intense study as a new way for material synthesis and potential commercial applications.[1–3] For further applications, attaching a third chemically distinct polymer chain to a diblock copolymer and forming a so-called ABC linear triblock copolymer make it possible to synergistically add functionality to the copolymer and to exploit more intricate morphologies that may not be accessible from that of diblock copolymers.[4–6] Recently, π-conjugated rigid-rod polymers with semiconducting properties have gained great interest since they possess unique optoelectronic properties with the potential to be used in flexible electronic devices, such as transistors,[7,8] photovoltaics,[9–11] and light-emitting diodes (LEDs),[12,13] *etc.* It is

[a]*Institute of Polymer Science and Engineering, National Taiwan University, Taipei, 10617, Taiwan. E-mail: polymer@ntu.edu.tw*
[b]*Department of Chemical Engineering, National Tsing-Hua University, Hsinchu, 30076, Taiwan*
[c]*Department of Chemistry, Tamkang University, Tamsui, 25137, Taiwan*
[d]*Department of Materials Science and Engineering, National Taiwan University, Taipei, 10617, Taiwan*
[e]*Department of Chemical Engineering, National Taiwan University, Taipei, 10617, Taiwan*

therefore of great interest to study triblock copolymer systems that combine a π-conjugated rod-like polymer with a coil–coil diblock copolymer for both academic research and industrial applications.

However, for a triblock copolymer system, there is a significant increase in the complexity of experimentally adjustable molecular parameters, which may include three different segment–segment interactions, two independent volume fractions, the degree of polymerization and the sequence of each constituent block for a complete understanding of its thermodynamic properties.[14–16] Recently, a simpler version to the triblock copolymer, a rod–coil type of diblock copolymer, has been synthesized and extensively investigated for its phase behavior.[17,18] It has now been shown that additional molecular characteristics, like the anisotropic rod–rod interaction and liquid crystalline behavior of the rod polymer, play a critical role in determining the actual boundary in the phase diagrams. On the theoretical side, self-consistent field theory[19] (SCFT) combined with the Maier–Saupe theory[20] and Landau expansion theory[21] have also been successful in predicting the microphase separation of rod–coil diblock copolymers. These studies reveal that rod–coil diblock copolymers may lead to a large region of lamellar phase.[11,22,23] In addition, a large number of intriguing self-assembly morphologies, such as wavy lamella,[17] zig-zag,[24] stripe-like[25] and puck-like[26,27] phases has also been discovered and closely correlated to the experimental observations.[28–32]

Recently, new triblock copolymer systems containing π-conjugated polymers have been developed for investigation of their morphology. For example, Lin *et al.* synthesized a new thermoresponsive triblock copolymer containing π-conjugated polyfluorene and studied its self-assembly behavior in the solution state.[33] Lee *et al.* investigated a coil–rod–coil triblock copolymer that organized into hexagonal column and spherical micelle liquid crystalline assemblies with different rod/coil volume ratios in the solid state.[34] In addition, by using a three-dimensional SCFT method, Xia *et al.* investigated the phase diagram for an ABC rod–coil–coil triblock copolymer.[35] Despite the aforementioned efforts, however, there has been only limited experimental study on the self-assembly behavior to establish the phase diagram of π-conjugated rod–coil–coil triblock copolymers in their solid state.

In this study, a new class of π-conjugated rod–coil–coil triblock copolymers of poly(diethylhexyloxy-*p*-phenylene vinylene)-*b*-poly(2-vinyl pyridine)-*b*-polystyrene (PPV-PVP-PS) was synthesized by coupling an end-functionalized PPV rod of a constant molecular weight with PS-PVP coil–coil diblock copolymers of different molecular weights and compositions. We aim to investigate the effect of the rod–rod interaction between π-conjugated PPVs on the self-assembly behavior of the PPV-P2VP-PS triblock copolymer by examining a series of PPV-PVP-PS triblock copolymers with PPV, PS, and PVP separately as the major component in the copolymers. In contrast to the complex non-lamellar structures formed by conventional ABC coil–coil–coil triblock copolymer systems, only lamellar phase was found for the series. By a combination of transmission electron microscopy (TEM) and simultaneously measured small-angle and wide-angle X-ray scattering (SAXS and WAXS) experiments on the thermally annealed PPV-PVP-PS samples, we discuss in detail the effect of the predominant rod–rod interactions between PPV chains on the formation of the resulting lamella structure.

Experimental section

Synthesis of PPV

Monodisperse poly (diethylhexyloxy-*p*-phenylene vinylene) (PPV) with an end-functionalized aldehyde for subsequent coupling reaction for the triblock copolymer synthesis was made by the Seigrist polycondensation method. Typical synthetic details for the polymer can be found in the literature.[29] The molecular parameters determined by using gel permeation chromatography (GPC) for the molecular weights and polydispersity and by using NMR for the end-group analysis are shown in Table 1.

Synthesis of the PPV-PVP-PS triblock copolymer

Three triblock copolymers of PPV-PVP-PS were synthesized by coupling the aforementioned aldehyde end-functionalized PPV rods of $M_n = 3800$ with living PS-PVP anion chains of different molecular weights. For the synthesis of PS-PVP living anions, a sequential anionic living polymerization was employed by using *sec*-butyllithium (*s*-BuLi, Aldrich, 1.3 M in cyclohexane) as an initiator in tetrahydrofuran (THF) at −78 °C for the polymerization. After styrene and 2-vinyl pyridine monomers were sequentially added in THF with a known amount of *s*-BuLi and allowed to polymerize for 30 mins and 2 h (Scheme 1(a)), respectively, one half of the resulting PS-PVP living anion was terminated with methanol and precipitated. The other half of the PS-PVP living anion was transferred to a reaction vessel filled with PPV dissolved in THF and used for the coupling reaction for the synthesis of the triblock copolymers (Scheme 1(b)). To ensure a complete coupling reaction of the transferred PS-PVP living anions with the aldehyde end-functionalized PPV macro-terminators, an excess amount of PPV (1.5 mol equiv.) with respect to the PS-PVP anions was used. The unreacted PPV can be easily removed by the precipitation of the triblock copolymer solution in hexane. After purification, the polydispersity index and the weight fraction of the PPV-PVP-PS triblock copolymer were evaluated using GPC and ^{1}H NMR, respectively. Results of the molecular characteristics of the triblock copolymers are listed in Table 1.

Small-angle and wide-angle X-ray scattering

All triblock copolymer samples were first melted at 210 °C for 10 mins to remove any prior thermal history followed by slow cooling them to 130 °C and annealing at this temperature for equilibrium for 2 days in a high vacuum environment (10^{-8} mmHg). The annealing temperature of 130 °C was chosen since it is above the glass transition temperature for all three PPV, PVP, and PS components to reach equilibrium. Simultaneous SAXS and WAXS measurements were performed at the SWAXS end-station (BL23A1 beamline) of the National Synchrotron Radiation Research Center (NSRRC) in Taiwan.

Transmission electron microscopy (TEM)

Triblock copolymer samples for the bulk morphology measurements using TEM were annealed following the same sample preparation procedure as that for SAXS and WAXS

Table 1 Molecular characteristics of PPV-PVP-PS triblock copolymers

Polymers	M_n PPV[a] (g mol^{-1})	M_n PVP[b] (g mol^{-1})	M_n PS[b] (g mol^{-1})	M_n Total (g mol^{-1})	PDI[b] Total	f_{PPV}[c]	f_{PVP}[c]	f_{PS}[c]	Morphology
PPV	3800	—	—	3800	1.20	—	—	—	smectic A
PVP-PS1	—	2400	2600	5000	1.08	—	0.48	0.53	disorder
PVP-PS2	—	2300	14 000	16 300	1.06	—	0.14	0.86	disordered micelles
PVP-PS3	—	11 000	6400	17 400	1.07	—	0.63	0.37	gyroid
PPV-PVP-PS1	3800	2400	2600	8800	1.12	0.43	0.27	0.30	triple-lamellae
PPV-PVP-PS2	3800	2300	14 000	20 100	1.16	0.19	0.11	0.70	broken triple-lamellae
PPV-PVP-PS3	3800	11 000	6400	21 200	1.14	0.18	0.52	0.30	broken triple-lamellae

[a] Measured by NMR. [b] Measured by GPC. [c] The volume fraction, f, of each block in the copolymers is calculated based on the density values of 0.99 g cm^{-3} for PPV, 1.01 g cm^{-3} for PS, and 1.04 g cm^{-3} for PVP.

measurements. A thin section of *ca.* 70 nm in thickness was cut from the annealed bulk specimen using a Reichert microtone with a diamond knife. Thin cut films were then exposed with iodine vapor for 8 h for staining PVP domains or with ruthenium tetroxide (RuO_4) vapor for 15 mins for staining PPV domains. TEM was performed using a JEOL1230 microscope operating at an accelerating voltage of 120 kV equipped with a Gatan CCD camera.

Polarizing optical microscopy (POM)

POM was carried out on a Zeiss Axio Imager A1m with a Mettler FP90/FP82HT hot stage system. The POM samples were pressed between two glass slides, and a constant nitrogen flow through the heating stage was upheld to prevent chemical decomposition. The samples were first heated to the isotropic state, and then cooled at a rate of 0.2 °C min^{-1} to observe the birefringent textures. To observe possible liquid crystallinity, the samples were sheared by sliding the cover slip to achieve orientation in the samples.

Results and discussion

First, we report the details on the morphological investigation of the thermally annealed π-conjugated rod–coil–coil PPV-PVP-PS triblock copolymer by employing TEM and SAXS. Fig. 1(a) shows the SAXS profiles for the PPV-PVP-PS1 triblock copolymer with PPV as the major species coupled with its low molecular weight symmetric PVP-PS1 diblock copolymer precursor. According to the SAXS profile, the broad and barely visible weak peak observed in the profile of the PVP-PS1 precursor is attributed to the effect of correlation hole resulted from the concentration fluctuations of the diblock copolymer in the disordered phase.[36,37] Because of its low molecular weight, the segregation strength χN of the PVP-PS1 precursor is less than the minimum for microphase separation of a value of 10.5 based on the mean-field theory prediction, where χ is the Flory-Huggin's interaction parameter and N is the overall degree of polymerization of the block copolymer. In a sharp contrast, however, the corresponding PPV-PVP-PS1 triblock copolymer shows strong scattering peaks at relative peak position ratios of 1 : 2 : 3 : 4 : 5 which correspond to a pattern for a microphase separated

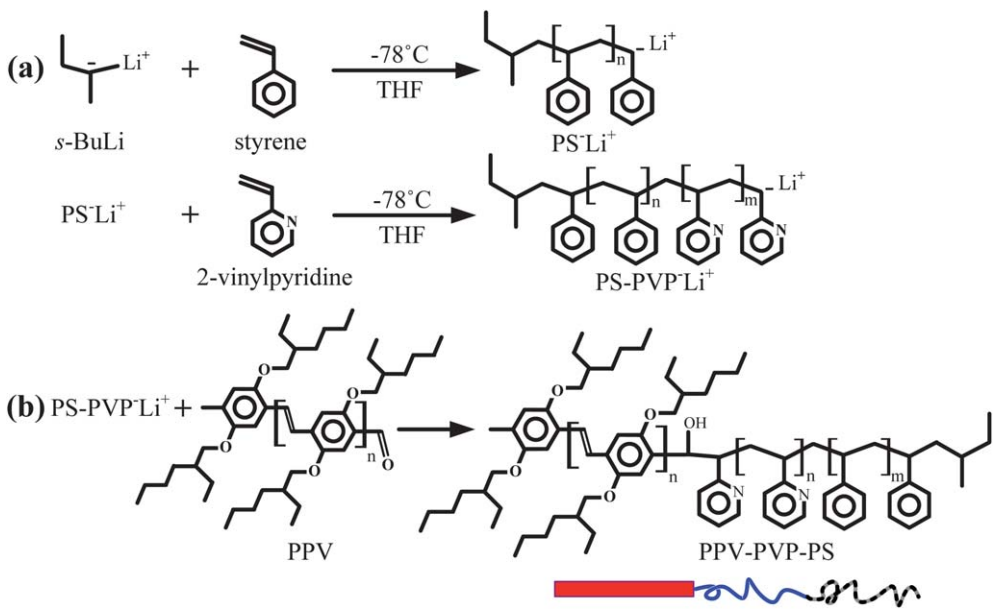

Scheme 1 (a) The synthetic scheme of a living PS-PVP lithium anion *via* sequential anionic polymerization. (b) The synthetic scheme of a PPV-PVP-PS triblock copolymer by coupling of the living PS-PVP lithium anion with an aldehyde end-terminated monodisperse PPV.

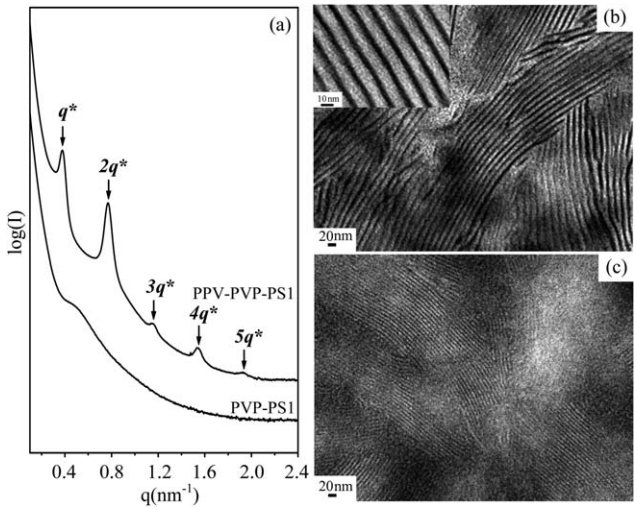

Fig. 1 (a) SAXS spectra for the PPV-PVP-PS1 triblock copolymer (upper curve) and its PVP-PS1 diblock precursor (lower curve). (b) A TEM micrograph of PPV-PVP-PS1 stained with RuO_4 shows a lamellar structure with a dark contrast corresponding to PPV domain. (c) A TEM micrograph of PPV-PVP-PS1 stained with iodine also shows a narrower spaced lamellar structure with a dark contrast corresponding to PVP domain.

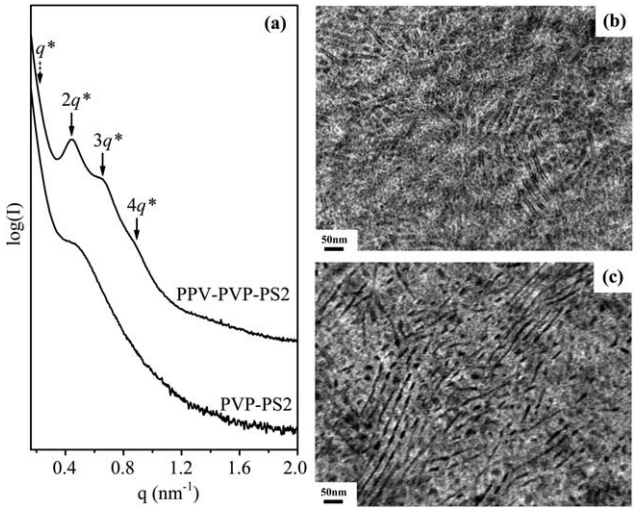

Fig. 2 (a) SAXS spectra for the PPV-PVP-PS2 triblock copolymer and for the PVP-PS2 precusor. (b) A TEM micrograph of the iodine-stained PPV-PVP-PS2 triblock copolymer shows a dark contrast strip, which corresponds to the PVP domain. (c) A TEM micrograph of the RuO_4-stained PPV-PVP-PS2 triblock copolymer shows a dark region corresponding to the PPV domain.

lamellar structure. From the first order peak position ($q^* = 0.38$ nm^{-1}, where q is the scattering wave vector), the long period spacing of the lamellar structure is found to be equal to 16.4 nm. Fig. 1(b) shows a transmission electron micrograph of the triblock copolymer stained with RuO_4 and the PPV domain exhibits as a dark lamellar layer in the micrograph. By directly measuring the width between the adjacent PPV domain centers on the micrograph, the measured width is approximately consistent with the long period spacing measured from the corresponding SAXS result shown in Fig. 1(a). In addition, the location of PVP domain within the lamellar structure can also be examined by using the iodine staining method. As shown in Fig. 1(c), the iodine-stained sample shows thinner but densely spaced dark lamellar layers which are in contrast with that from the sample stained with RuO_4 for the PPV domains. Since iodine can only stain PVP segments in the sample, the iodine-stained TEM micrograph indicates that the midblock PVP is fully microphase separated from the PPV domain as well as from the PS domain. On the basis of these two staining methods, it is clear that a self-assembling morphology of triple-lamellar phase is induced after PPV rods are attached on the otherwise single phase PVP-PS1 diblock copolymer.

The phase behavior of the PPV-PVP-PS rod–coil–coil triblock copolymer is further examined by changing the copolymer composition. For PS-rich PPV-PVP-PS2, the molecular weight of its PS block is increased significantly compared with that of the PS block in PPV-PVP-PS1, while the molecular weight of both the PPV and PVP blocks remain roughly constant for the two samples. The corresponding SAXS patterns of PPV-PVP-PS2 and its coil precursor PVP-PS2 are shown in Fig. 2(a). Similar to that of PVP-PS1, a relatively broad and weak peak is observed in the profile for the PVP-PS2 diblock precursor, also indicating an isotropic or a disordered micelle phase. The formation of the disordered micelle phase may be due to the relatively low volume fraction of the PVP block ($f_{PVP} = 0.14$) as well as a relatively low overall molecular weight (~16 000 g mol^{-1}) of PVP-PS2. However, as this compositionally asymmetric PVP-PS2 precursor is attached onto the PPV rod to form a π-conjugated rod–coil–coil triblock copolymer, it can be seen that even though the PPV-PVP-PS2 has a relatively low PPV volume fraction of only 0.19, the SAXS profile of the PPV-PVP-PS2 triblock copolymer shows a scattering pattern with relative peak positions in the ratio of 2 : 3 : 4, likely indicating a microphase separated lamellar structure. However, there appears to be a complete disappearance of the first order peak in the SAXS profile for PPV-PVP-PS2. Generally, it is not common to observe the missing of the first order scattering peak in the SAXS pattern for a self-assembling diblock copolymer system with two different electron densities. In contrast, the result of the disappearance of the first scattering peak for a triblock lamellar system could be due to the scattering from the following two cases; one is that there are at least three different self-organized lamellar layers with the electron density of the middle layer either higher or lower than that of the two neighboring layers; and the other is from three self-organized lamellae with one layer's electron density apparently larger than the others.[3,38] A similar SAXS pattern with the first order scattering peak missing has also been previously reported on a polystyrene-*b*-poly(2-vinylpyridine)-*b*-poly(*tert*-butyl methacrylate) triblock copolymer system in which the middle PVP block has the highest electron density.[38] It works in the same fashion with regard to the missing first scattering peak in our system since the electron density of the middle PVP block ($\rho_e = 0.611$mole cm^{-3}) is also higher than that of two end blocks of PS (0.566 mole cm^{-3}) and PPV (0.553 mole cm^{-3}). Therefore, we could observe the disappearance of the first order peak in the SAXS pattern for the PPV-PVP-PS systems. Typically, the long period spacing of a lamellar structure of a block copolymer system can be calculated from the first order scattering peak position in the SAXS pattern. For PPV-PVP-PS2, the long period spacing of its lamellar structure can be

calculated from the q value of the second order peak divided by two ($2q^*/2 = 0.23$ nm^{-1}), which corresponds to the real long spacing of 27.3 nm.

Furthermore, TEM can also be used to provide important information about how PPV-PVP-PS might be organized within its nanostructure. As shown in Fig. 2(b) for PPV-PVP-PS2, the PVP domain stained with iodine showing a dark contrast in the micrograph reveals the complete phase separation of the PVP domain from that of the PS and PPV blocks. Moreover, PPV-PVP-PS2 stained in the PPV domain with RuO_4 shows only disrupted and short-range dark lines of the PPV domain with morphology that is in great contrast with that of the PPV-PVP-PS1, in which case a long-range ordered lamellar structure was observed. Therefore, combining the SAXS result from Fig. 2(a) and the TEM study from Fig. 2(b) and 2(c), PPV-PVP-PS2 exhibits a so-called broken triple-lamellar phase with disrupted short PPV layers. In addition, the distance between the centers of the two stained PPV domains can be estimated from Fig. 2(c), which is 25 ± 2 nm, a value that is in good agreement with the long period spacing measured from the corresponding SAXS result (27.3 nm).

PPV-PVP-PS3 is the rod–coil–coil triblock copolymer with PVP as its major species and it has a low PPV volume fraction of only 0.18. Fig. 3(a) shows the corresponding SAXS profiles of PPV-PVP-PS3 and its PVP-PS3 diblock precursor. Compared to the disordered phase exhibited by PVP-PS1 and PVP-PS2 due to the low degree of polymerization and the highly compositional asymmetry, respectively, for phase separation, PVP-PS3 diblock precusor with a higher overall degree of polymerization exhibits scattering reflections in the q space in ratios of $\sqrt{3}$, $\sqrt{4}$, $\sqrt{11}$, $\sqrt{23}$, $\sqrt{27}$, corresponding to a bicontinuous gyroid structure. Generally, the complex bicontinuous gyroid structure can be found to exist in a narrow composition window between the classical lamella and hexagonal packed cylinder morphologies in conventional coil–coil diblock copolymer systems. PVP-PS3 with the PS volume fraction $f_{PS} = 0.37$ is located in this narrow window for the formation of a gyroid phase. The synthesis of the corresponding PPV-PVP-PS3 allows us to investigate the effect of PPV addition to the highly curvaceous ordered structure of PVP-PS3 on the resulting morphology of the PPV-PVP-PS3 system. Similar to the SAXS patterns observed for PPV-PVP-PS1 and PPV-PVP-PS2, the SAXS profile of the PPV-PVP-PS3 triblock copolymer also shows the scattering maxima at relative positions of 1 : 2 : 3 : 4 : 6, which again corresponds to the reflections of a microphase-separated lamellar structure. The result of a smaller first order peak intensity than that of its second peak in the SAXS profile is also resulted from the similar aforementioned effect caused by the higher electron density from the middle high molecular weight PVP block than that of the two end blocks PS and PPV. From the q value of the first order peak ($q^* = 0.22$ nm^{-1}), the long period spacing of the corresponding lamellar structure is found to be equal to 28.6 nm. Similar to the TEM observation for PPV-PVP-PS2 with PS as its major component, a broken triple-lamellar phase of PPV-PVP-PS3 with PVP as its major component has also been observed as shown in Fig. 3(b) and 3(c).

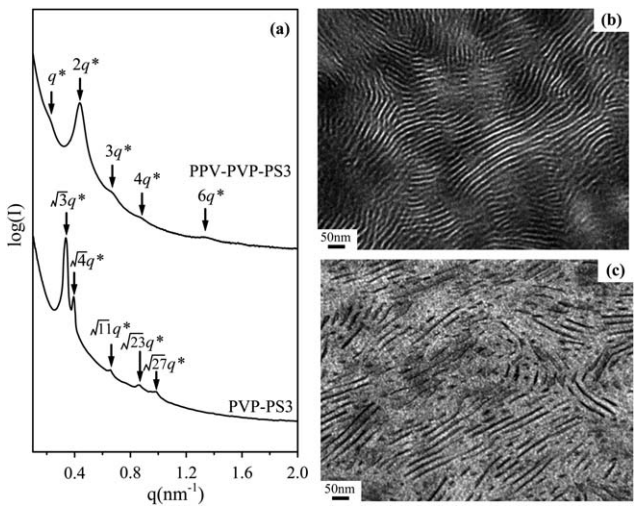

Fig. 3 (a) SAXS spectra for the PPV-PVP-PS3 triblock copolymer and the PVP-PS3 precusor. (b) A TEM micrograph of the iodine-stained PPV-PVP-PS3 triblock copolymer shows a dark region which corresponds to the PVP nanodomain. (c) A TEM micrograph of the RuO_4-stained PPV-PVP-PS3 triblock copolymer shows a dark region corresponding to PPV nanodomains.

It has been known for a rod–coil diblock copolymer system containing π-conjugated segments that there are several ways by which PPVs may adopt to pack themselves within their lamellar domain, *e.g.* forming a monolayer or a bilayer of PPV lamellae.[30] To further investigate the PPV molecular packing in the triple lamellar phase, we introduce a method to determine the one-dimensional (1-D) electron density profile across the lamellar structure using the following equation:[39,40]

$$\rho_e(z) \sim \sum_{k=1}^{n} \sqrt{I(q_k)q_k^2}\ \phi_k \cos(q_k z) \quad (1)$$

where n is the total number of diffraction order peaks appeared in the SAXS spectrum, q_k is the scattering vector of the kth diffraction order peak position, $\sqrt{I(q_k)q_k^2}$ is the magnitude of the kth scattering wave amplitude, and φ_k is the phase of the scattering wave, which can take the value of either +1 or −1 for a centrosymmetical lamellar structure. The conversion of the 1-D electron density profile is first conducted from the SAXS spectrum for the PPV-PVP-PS1 using eqn (1). As shown in Fig. 4(a), the regular scattering intensity *vs.* scattering wavevector, q, is replotted as the Lorentz-corrected profile in which Iq^2 is plotted against q to obtain the magnitude of the kth amplitude of the scattering wave. The Lorentz-corrected profile again exhibits a unique feature that the magnitude of the first order peak is weaker than that of the second one. As shown in Fig. 4(b), the relative 1-D electron density profile of PPV-PVP-PS1 was calculated based on eqn (1) by using the magnitudes of the first four scattering peak intensities shown in Fig. 4(a) and by combining a suitable choice of a relative phase between the first four scattering peaks with $\varphi_k = -1, -1, +1$, and +1, for $k = 1, 2, 3$ and 4, respectively. The deepest valley region centered at $z = 0$ corresponds to the PPV rod layer with the lowest electron density, while the two peaks centered at $z = \pm 4.5$ nm represent the region of the PVP domains with the highest electron density. The shallower valley region centered at $z = \pm 7.7$ nm correspond to the PS layer and the distance between the center of the two

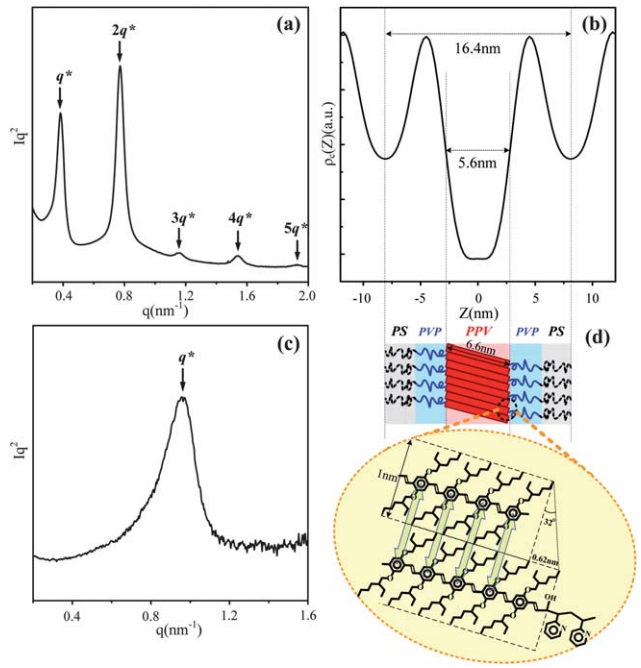

Fig. 4 (a) The Lorentz-corrected profile (Iq^2 *vs.* q) and (b) the relative density profile of the PPV-PVP-PS1 triblock copolymer. (c) The Lorentz-corrected profile of the homopolymer PPV precursor. (d) A schematic representation of the molecular packing of the PPV-PVP-PS1 triblock copolymer in the triple lamellar phase.

shallower valleys is approximately equal to 16.5 nm, which is roughly the same value corresponding to the long spacing of the triple-lamellar structure of PPV-PVP-PS1 measured from the TEM result. Besides, the thickness of the PPV rod layer in the triple-lamellar structure, which can be estimated based on the distance between the two half maximum points of the slope of the deepest valley curve in the 1-D electron density profile, is *ca.* 5.6 nm. To identify the orientation of PPV rods within their domain, a SAXS measurement on the pristine homopolymer PPV precursor was conducted to obtain its fully extended rod length. As shown in Fig. 4(c), a peak of the pure homopolymer PPV, which corresponds to the layering structure of PPV rods, is visible at $q = 0.95$ nm^{-1}, indicating the formation of a smectic A phase of the monodisperse homopolymer PPV.[41] Based on the Braggs' equation, the chain length of the PPV rod was estimated to be *ca.* 6.6 nm. Because the thickness of the PPV domain in the triple-lamellar phase (5.6 nm) is smaller than the fully extended chain length of the pristine homopolymer PPV rod (6.6 nm), the PPV rods in the triple-lamellar phase of PPV-PVP-PS1 must be tilted with respect to the lamellae layer normal, thus leading to an average tilt angles of either 32° or 67°, corresponding to two possible packings of a smectic C monolayer or a smectic C bilayer, respectively. It has also been reported by Sary *et al.* on a rod–coil diblock copolymer system containing PPV that, since the minimization of the inter-distance between PPV monomer units for an optimum interaction, only a discrete tilt angle was allowed.[30] As shown in Fig. 4(d), by the combination of the above results of the fixed tilt angle of 32° and the estimate of the diameter of PPV rod to be ~1 nm, a mismatch between adjacent PPV rods along the PPV domain of 0.63 nm was calculated, which approximately corresponds to the expected value of one displaced PPV monomer unit of ~0.66 nm.[42] Therefore, an organization of the smectic C monolayer in PPV domain is proposed here since it is more likely than the assumption of the organization of a smectic C double layer with a shift of 2.36 fractional repeated units of the monomers between adjacent PPV rods. By a combination of the above results obtained from SAXS, TEM, and the 1-D electron density profile, a schematic representation of the molecular packing of PPV-PVP-PS1 within its long period of the triple-lamellar structure is shown in Fig. 4 (d). The smectic C organization of PPV-PVP-PS1 was also confirmed by the detection of blurred Schlieren textures (Fig. 5 (a)) under a polarizing optical microscope upon cooling at 140 °C. It is worth noting that PPV-PVP-PS1 can be easily aligned to show homogenous streak texture when sandwiched between glass slides with shear (Fig. 5(b)).

Phase transitions

Since the anisotropic rod–rod interaction between π-conjugated PPV was found to be temperature dependant,[43] simultaneously measured SAXS and WAXS experiments as a function of temperatures were performed to investigate the effect of temperature on the self-assembling behavior and on the solid and liquid crystalline structures of the triblock copolymers. The WAXS measurements were used to characterize the molecular packing of PPV chains within the microphase separated domains

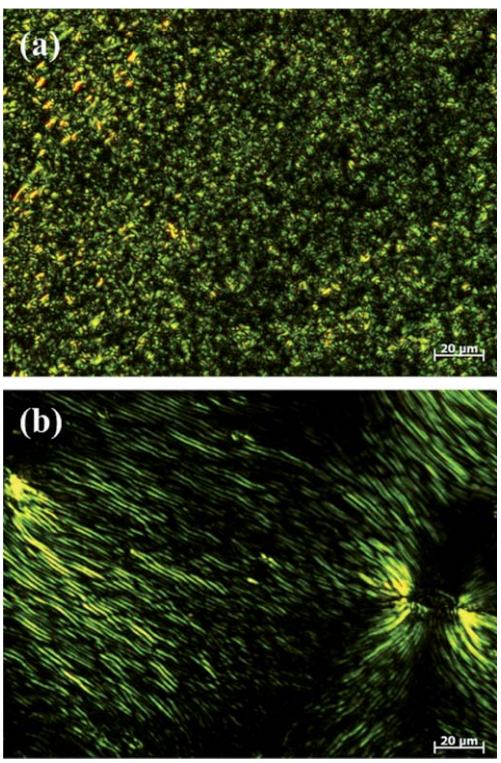

Fig. 5 Micrographs showing liquid crystalline smectic C textures of PPV-PVP-PS1 under a polarizing optical microscope at 140 °C upon cooling. (a) The blurred Schlieren texture of a sample without the cover glass and (b) a texture of Schlieren and streaks for a sample sandwiched between slides.

as a function of temperatures between room temperature and 190 °C, at which all crystalline peaks of PPV disappear. First, as shown in Fig. 6(b) of the WAXS spectrum of PPV-PVP-PS1 at room temperature, the first peak located at around 6.5 nm^{-1} corresponds to the lateral spacing between PPV rods. The assignment for the crystalline plane for each diffraction peak shown in Fig. 6(b) is based on the previous detailed X-ray study on the PPV homopolymer by Segalman *et al.*[42] Upon heating from the ambient temperature to 80 °C for PPV-PVP-PS1, a significant increase in the diffraction intensity and the sharpening of these peaks indicate a melting transition of PPV rod from its solid crystalline phase into a smectic liquid crystalline phase, which improves the alignment between PPV rods in their domain. In addition, during the step-wise in-line heating of the sample, a continuous shift of the first peak towards low q demonstrates an increase in the PPV rod–rod lateral spacing, which can be attributed to the thermal expansion of the PPV rods upon heating.

The results of the evolution in the SAXS profiles with temperatures shown in Fig. 6(a) demonstrates that the characteristic scattering peaks corresponding to the self-assembled triple-lamellar phase decrease in intensity and all peak intensities disappear completely at 190 °C, indicating the occurrence of the phase transition from the lamellae phase to a disordered phase. Concurrently, the WAXS diffraction peaks associated with the liquid crystalline structure between PPV rods also disappear completely at 190 °C, indicating a smectic/isotropic transition, as shown in Fig. 6(b). Therefore, the triblock copolymer undergoes the ordered lamella-to-disorder transition and the smectic/isotropic transition at the same temperature. In addition, the above results show that the presence of the rod–rod interactions between PPV blocks may have the dominating effects both on the formation as well as on the stabilization of the lamellar structure of PPV-PVP-PS1 to exist at temperatures below 190 °C. Furthermore, upon heating the sample to a temperature just around 160 °C, the intensity of the second order peak in the Lorentz-corrected SAXS profile of PPV-PVP-PS1 (result not shown) drops below that of its first order peak, which corresponds to a diffraction pattern common to that from a two-layer lamellar structure. The 1-D electron density profile of PPV-PVP-PS1 at 170 °C as depicted in Fig. 7(a) shows indeed a two-layer lamellar structure, which indicates that both PS and PVP blocks with higher electron density among the three species form one single miscible layer and that the PPV rods, having the dominating rod–rod interaction, form the other layer in this double-lamellar structure at this temperature. Therefore, a phase transformation from the original low-temperature ($T \leqq 170$ °C) triple-lamellar phase to a high-temperature (190 °C > $T \geqq$ 170 °C) double-lamellar phase consisting of a layer of PPV rods and a homogeneous PS and P2VP layer was observed, as schematically illustrated in Fig. 7(b). Upon further heated above 190 °C, the PPV-PVP-PS1 triblock copolymer exhibits no observable peaks in both SAXS and WAXS spectra, indicating that the triblock copolymer transforms into a single disordered phase with no liquid crystalline structure. Recently, Xia *et al.*[35] reported a self-consistent mean field theory (SCFT) calculation on the self-assembly of linear ABC rod–coil–coil triblock copolymers in three-dimensional space. They predicted a similar phase transition from an alternating triple-lamellar phase to a double-lamellar phase near the order–disorder transition temperature (T_{ODT}) as the triblock copolymer consists of roughly equal length of A and B coil blocks, and the volume fraction of a C rod block is around 0.4, with a composition which is similar to our system. Their result is in good agreement with our experimental findings.

Fig. 8(a) and 8(b) show the evolution of SAXS and WAXS patterns, respectively, as a function of temperature for PS-rich PPV-PVP-PS2. Similar to the result of the PPV-PVP-PS1, the characteristic scattering peaks corresponding to the self-assembled lamellar phase of PPV-PVP-PS2 disappear simultaneously

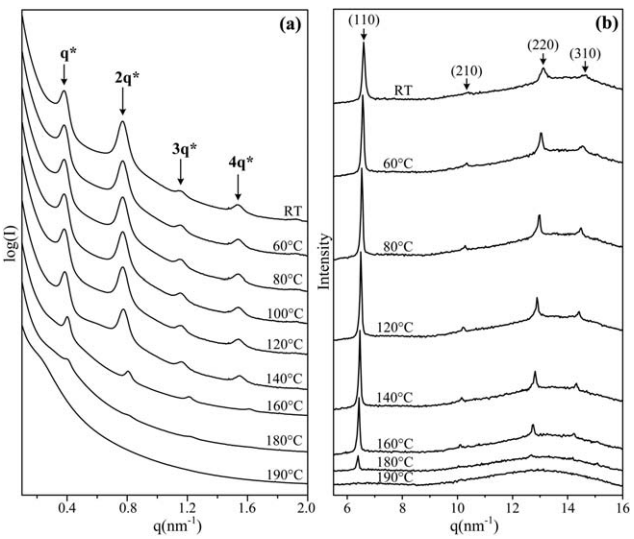

Fig. 6 Simultaneously measured (a) SAXS and (b) WAXS spectra as a function of temperature for the PPV-PVP-PS1 triblock copolymer.

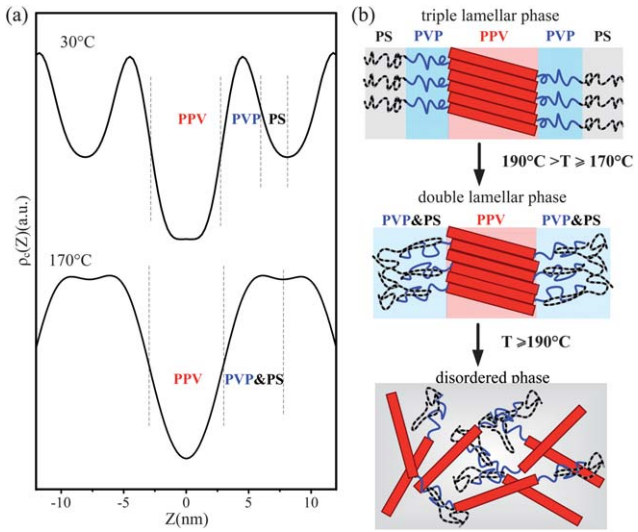

Fig. 7 (a) The 1-D electron density profiles extracted from the SAXS pattern (Fig. 5(a)) of the PPV-PVP-PS1 triblock copolymer at 30 °C and 170 °C. (b) Sequential phase transformations from the triple-layer lamellar structure to a double-layer lamellar structure and finally to a disordered phase for the PPV-PVP-PS1 triblock copolymer were observed with increasing temperature.

with the disappearance of the anisotropic rod–rod interaction between PPV at 190 °C, as indicated by the complete disappearance of the major (110) peak. Therefore, PPV-PVP-PS2 also forms a single amorphous disordered phase above 190 °C. A similar phase transition for PPV-PVP-PS3 is also observed at the same temperature, as shown in Fig. 9(a) and 9(b) of its SAXS and WAXS patterns as a function of temperature. However, in contrast to the PPV-PVP-PS1 and PPV-PVP-PS2, a new peak near the low q range around 0.38 nm^{-1} suddenly emerges for PPV-PVP-PS3 when it is heated above 190 °C. Therefore, at 190 °C, only this new and relatively broad peak remains but the primary peak originating from the lamellae structure disappears. The formation of the broad and weak peak at $T \geqq 190$ °C is suspected to be due to the effect of the correlation hole resulted from the concentration fluctuations of the triblock copolymer in the disordered phase in which all three PPV, PVP and PS blocks are homogeneous above $T = 190$ °C. A TEM micrograph for a PPV-PVP-PS3 sample heated to 200 °C is shown in Fig. 10. The sample stained with iodine to show PVP in dark contrast in the micrograph exhibits a disordered structure of the triblock copolymer. In addition, the disappearance of the primary peak in SAXS patterns coincides with the disappearance of the major WAXS diffraction peak at exactly the same temperature. Therefore, the formation and the stability of the triple-lamellar phase are closely related to the rod–rod interactions between the PPV rod segements.

Formation of triple-lamellar phase

The striking result for the formation of the triple lamellar phase for all triblock copolymers with vastly different rod and coil fractions can be compared with those from ABC coil–coil–coil triblock counterparts. For coil–coil–coil triblock copolymers with three chemically different species, unusually complex

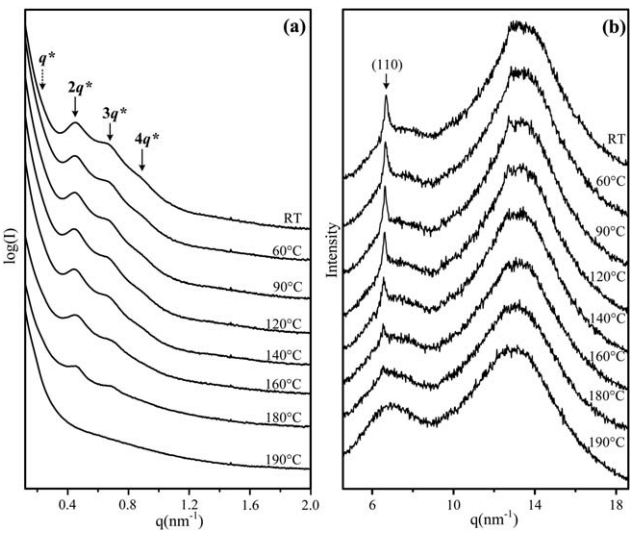

Fig. 8 Simultaneously measured (a) SAXS and (b) WAXS spectra as a function of temperature for the PPV-PVP-PS2 triblock copolymer. The complete disappearance of the first order peak in the SAXS spectra indicated by a dashed arrow marked with q^* results from the cancellation of the scattering of the lamellar structured triblock copolymer of PPV-PVP-PS2 with the highest electron density in the PVP midblock.

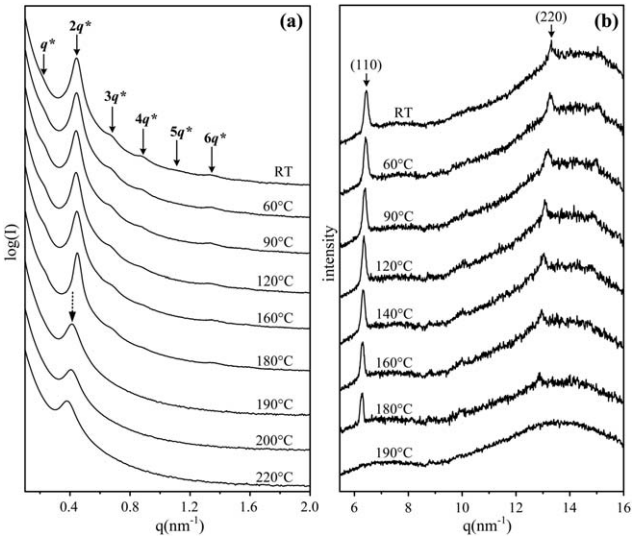

Fig. 9 Simultaneously measured (a) SAXS and (b) WAXS spectra as a function of temperature for the PPV-PVP-PS3 triblock copolymer. A dashed arrow is added to indicate the emergence of a new peak in the SAXS spectra associated with scattering from the "correlation hole" from the disordered phase of PPV-PVP-PS3 heated above 190 °C.

structures in addition to the classical structures for AB coil–coil diblock copolymers of sphere, cylinder, gyroid, and lamella have been theoretically predicted, as well as experimentally discovered. For example, with the midblock B strongly disliked by the two end blocks, Stadler *et al.* have demonstrated that new structures of "cylinder at the wall" and "ball at the wall" morphologies can be observed, depending on the copolymer composition.[4] Recently, Tang *et al.* constructed a complete phase diagram in the strong segregation regime for an ABC linear coil–coil–coil triblock copolymer using the self-consistent mean field calculation method.[44] They have also discovered that additional complex non-lamellar structures like the lamellae with beads at the interface and hexagonal phase with beads at the interface, *etc.* were resulted where the Flory-Huggins interaction parameters for A, B, and C segments have a relationship of $\chi_{A-B} \approx \chi_{B-C} > \chi_{A-C}$. For our current PPV-PVP-PS system, since PVP is rather polar due to its pyridine unit yet PPV and PS are non-polar

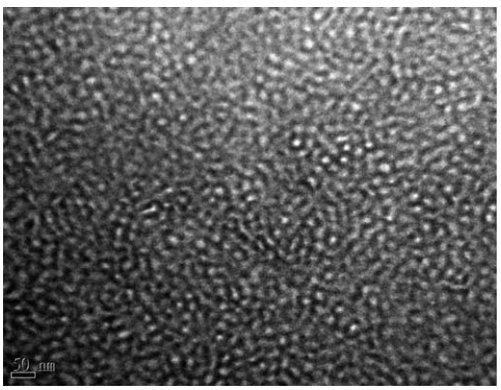

Fig. 10 A TEM micrograph of PPV-PVP-PS3 stained with iodine that shows a disordered phase of the copolymer at 200 °C.

polymers, the midblock PVP is also strongly disliked by two the end PPV and PS blocks. In addition, based on an earlier detailed study on the self-assembly behavior of a PPV-PS rod–coil diblock copolymer system,[30] Sary *et al.* showed that the block copolymer displayed an equilibrium isotropic structure, indicating that the Flory-Huggins interaction between PPV and PS was also expected to be rather small. Therefore, the relationship between the three Flory-Huggins interaction parameters for our PPV-PVP-PS system can be approximated as $\chi_{PPV-PVP} \approx \chi_{PVP-PS} > \chi_{PPV-PS}$, which can be approximated to the same thermodynamic criteria for which a non-lamellar phase may prevail for coil–coil–coil triblock copolymer systems. Therefore, we would have also expected that the current PPV-PVP-PS system might exhibit many non-lamellar structures with different copolymer compositions if PPVs were to behave as a coil-like polymer chain with no lateral rod–rod interaction. This is not what we have observed in the current study. The morphology difference between ABC rod–coil–coil and coil–coil–coil triblock copolymers strongly suggests that the anisotropic rod–rod interaction between PPV rods plays a dominant role on the formation of the observed triple-lamellar structure.

In addition, the formation of the triple lamellar phase for PPV-PVP-PS1 requires more discussion since we would have expected that PPV-PVP-PS1 with $f_{PPV} = 0.43$ exhibited a two-layer lamellar structure with its PPV blocks forming one layer and its single-phase PVP-PS1 alone forming the other homogenous layer in the lamellar structure.[31,32] However, the formation of a PPV lamellae domain surface may be regarded to serve as an impenetrable surface that pins the connected PVP-PS1 chains as a highly stretched end-anchoring polymer brush on the PPV surface, leading to the formation of three distinct PPV, PVP and PS layers. Similarly, PS-rich PPV-PVP-PS2 and PVP-rich PPV-PVP-PS3 also exhibit the triple-lamellar structure, even though their PPV volume fraction is less than 0.2. This result for the formation of triple lamellar structure for the current triblock copolymer system is also in a sharp contrast with that of many PPV-based rod–coil diblock copolymer systems at similar rod-fractions in which non-lamellae phases, *e.g.* hexagonal packed structure, were observed.[28,32] Therefore, the rod block in triblock copolymer systems leads to an even larger region of lamellar phase compared with that from diblock copolymers containing PPV. With increasing the molecular weight of either PVP or PS, the formation of a highly ordered triple-lamellae phase for PPV-PVP-PS2 and PPV-PVP-PS3 systems may lead to an increase in the free energy due to an excess of chain stretching of their PS and PVP blocks. Therefore, the formation of a broken triple-lamellar phase is observed for the PPV-PVP-PS2 and PPV-PVP-PS3 systems since the penalty associated with chain stretching of the anchored PS-PVP coils can be reduced if a short PPV lamellae structure is formed, leading to the broken lamellar phase. In light of the current experimental results, more theoretical work is needed in order to fully understand such an effect of the rod–rod interaction on ABC triblock copolymer systems containing π-conjugated segments in the future.

Conclusions

In conclusion, ABC linear rod–coil–coil triblock copolymers containing one end-block of a PPV rigid rod with strong rod–rod interactions and two coil blocks of different compositions were synthesized. TEM and simultaneous SAXS/WAXS measurements as a function of temperature were used to investigate the effect of the rod–rod interaction and the composition on the self-assembly behavior of the synthesized triblock copolymers. In sharp contrast to coil–coil–coil triblock copolymers with compositional asymmetry that display many intricate non-lamellar self-assemble structures, all three π-conjugated rod–coil–coil triblock copolymers with vastly different rod fractions and coil compositions exhibit a triple-lamellar structure with each domain corresponding to the constituent block. Upon heating, the lamellar structure persists up to 180–190 °C, at which the triblock copolymers undergo both the order-to-disorder transition as well as the liquid crystalline-to-isotropic transition, a strong evidence that shows rod–rod interactions between PPV plays a key role in the formation and the stabilization of the lamellar structure. The finding is consistent with recent theoretical predictions based on mean-field calculations. The results we present here may provide some insight to explore the phase behavior in more complex multiblock copolymer systems with π-conjugated segments in the future.

Acknowledgements

The financial support from National Science Council of Taiwan is greatly appreciated. The X-ray measurements were conducted in Taiwan at the National Synchrotron Radiation Research Center. The authors also like to thank Prof. Rachel A. Segalman for her helpful discussion on the work.

References

1 F. S. Bates and G. H. Fredrickson, *Phys. Today*, 1999, **52**, 32–38.
2 J. Chatterjee, S. Jain and F. S. Bates, *Macromolecules*, 2007, **40**, 2882–2896.
3 G. G. du Sart, I. Vukovic, G. A. van Ekenstein, E. Polushkin, K. Loos and G. ten Brinke, *Macromolecules*, 2010, **43**, 2970–2980.
4 U. Krappe, R. Stadler and I. Voigtmartin, *Macromolecules*, 1995, **28**, 4558–4561.
5 R. Stadler, C. Auschra, J. Beckmann, U. Krappe, I. Voigtmartin and L. Leibler, *Macromolecules*, 1995, **28**, 3080–3097.
6 U. Breiner, U. Krappe, E. L. Thomas and R. Stadler, *Macromolecules*, 1998, **31**, 135–141.
7 C. D. Dimitrakopoulos and P. R. L. Malenfant, *Adv. Mater.*, 2002, **14**, 99.
8 M. L. Chabinyc and A. Salleo, *Chem. Mater.*, 2004, **16**, 4509–4521.
9 K. M. Coakley and M. D. McGehee, *Chem. Mater.*, 2004, **16**, 4533–4542.
10 H. Hoppe and N. S. Sariciftci, *J. Mater. Res.*, 2004, **19**, 1924–1945.
11 W.-C. Yen, Y.-H. Lee, J.-F. Lin, C.-A. Dai, U.-S. Jeng and W.-F. Su, *Langmuir*, 2011, **27**, 109–115.
12 R. H. Friend, R. W. Gymer, A. B. Holmes, J. H. Burroughes, R. N. Marks, C. Taliani, D. D. C. Bradley, D. A. Dos Santos, J. L. Bredas, M. Logdlund and W. R. Salaneck, *Nature*, 1999, **397**, 121–128.
13 A. J. Heeger, *Angew. Chem., Int. Ed.*, 2001, **40**, 2591–2611.
14 S. I. Stupp, V. LeBonheur, K. Walker, L. S. Li, K. E. Huggins, M. Keser and A. Amstutz, *Science*, 1997, **276**, 384–389.
15 T. A. Shefelbine, M. E. Vigild, M. W. Matsen, D. A. Hajduk, M. A. Hillmyer, E. L. Cussler and F. S. Bates, *J. Am. Chem. Soc.*, 1999, **121**, 8457–8465.
16 T. S. Bailey, H. D. Pham and F. S. Bates, *Macromolecules*, 2001, **34**, 6994–7008.
17 J. T. Chen, E. L. Thomas, C. K. Ober and G. P. Mao, *Science*, 1996, **273**, 343–346.
18 S. A. Jenekhe and X. L. Chen, *Science*, 1999, **283**, 372–375.
19 M. W. Matsen and M. Schick, *Phys. Rev. Lett.*, 1994, **72**, 2660–2663.

20 V. Pryamitsyn and V. Ganesan, *J. Chem. Phys.*, 2004, **120**, 5824–5838.
21 R. Holyst and M. Schick, *J. Chem. Phys.*, 1992, **96**, 730–740.
22 P. Tang, W. D. Song, F. Qiu, Y. L. Yang and A. C. Shi, *J. Phys. Chem. B*, 2011, **115**, 8390–8400.
23 P. Tang, W. D. Song, H. D. Zhang, Y. L. Yang and A. C. Shi, *Macromolecules*, 2009, **42**, 6300–6309.
24 J. T. Chen, E. L. Thomas, C. K. Ober and S. S. Hwang, *Macromolecules*, 1995, **28**, 1688–1697.
25 L. H. Radzilowski, B. O. Carragher and S. I. Stupp, *Macromolecules*, 1997, **30**, 2110–2119.
26 J. H. Ryu, N. K. Oh, W. C. Zin and M. Lee, *J. Am. Chem. Soc.*, 2004, **126**, 3551–3558.
27 B. K. Cho, Y. W. Chung and M. Lee, *Macromolecules*, 2005, **38**, 10261–10265.
28 B. D. Olsen and R. A. Segalman, *Macromolecules*, 2007, **40**, 6922–6929.
29 B. D. Olsen and R. A. Segalman, *Macromolecules*, 2005, **38**, 10127–10137.
30 N. Sary, R. Mezzenga, C. Brochon, G. Hadziioannou and J. Ruokolainen, *Macromolecules*, 2007, **40**, 3277–3286.
31 N. Sary, L. Rubatat, C. Brochon, G. Hadziioannou, J. Ruokolainen and R. Mezzenga, *Macromolecules*, 2007, **40**, 6990–6997.
32 C.-C. Ho, Y.-H. Lee, C.-A. Dai, R. A. Segalman and W.-F. Su, *Macromolecules*, 2009, **42**, 4208–4219.
33 S. T. Lin, K. Fuchise, Y. G. Chen, R. Sakai, T. Satoh, T. Kakuchi and W. C. Chen, *Soft Matter*, 2009, **5**, 3761–3770.
34 M. Lee, D. W. Lee, B. K. Cho, J. Y. Yoon and W. C. Zin, *J. Am. Chem. Soc.*, 1998, **120**, 13258–13259.
35 Y. D. Xia, J. Z. Chen, Z. Y. Sun, T. F. Shi, L. J. An and Y. X. Jia, *Polymer*, 2010, **51**, 3315–3319.
36 L. Leibler, *Macromolecules*, 1980, **13**, 1602–1617.
37 B. Nandan, C. H. Lee, H. L. Chen and W. C. Chen, *Macromolecules*, 2005, **38**, 10117–10126.
38 S. Ludwigs, A. Boker, V. Abetz, A. H. E. Muller and G. Krausch, *Polymer*, 2003, **44**, 6815–6823.
39 C. M. Wu, W. Liou, H. L. Chen, T. L. Lin and U. S. Jeng, *Macromolecules*, 2004, **37**, 4974–4980.
40 S. C. Chen, S. W. Kuo, U. S. Jeng, C. J. Su and F. C. Chang, *Macromolecules*, 2010, **43**, 1083–1092.
41 B. D. Olsen, S. Y. Jang, J. M. Luning and R. A. Segalman, *Macromolecules*, 2006, **39**, 4469–4479.
42 B. D. Olsen, D. Alcazar, V. Krikorian, M. F. Toney, E. L. Thomas and R. A. Segalman, *Macromolecules*, 2008, **41**, 58–66.
43 B. D. Olsen, M. Shah, V. Ganesan and R. A. Segalman, *Macromolecules*, 2008, **41**, 6809–6817.
44 P. Tang, F. Qiu, H. D. Zhang and Y. L. Yang, *Phys. Rev. E: Stat., Nonlinear, Soft Matter Phys.*, 2004, **69**.

